THE JOURNAL OF PHYSICAL CHEMISTRY Letters

Letter

Cite This: J. Phys. Chem. Lett. 2019, 10, 799−805

pubs.acs.org/JPCL

Weak Interactions in Alkaline Earth Metal Dimers by Pair-Density Functional Theory

Jie J. Bao, Laura Gagliardi,* and Donald G. Truhlar*

Department of Chemistry, Chemical Theory Center, and Supercomputing Institute, University of Minnesota, Minneapolis Minnesota 55455-0431, United States

Supporting Information

ABSTRACT: Alkaline earth dimers have small bond energies (less than 5 kcal/mol) that provide a difficult challenge for electronic structure calculations. They are especially challenging for Kohn−Sham density functional theory (KS-DFT) using generalized gradient approximations (GGAs) as the exchange−correlation density functional because GGAs often do not provide accurate results for weak interactions. Here we treat alkaline earth dimers from six different rows of the periodic table. We show that the dominant correlating configurations are the same in all six dimers. We also show that multiconfiguration pair-density functional theory (MC-PDFT) using a fully translated GGA as the on-top density functional not only performs much better than KS-DFT with GGAs in predicting equilibrium distances and dissociation energies but also performs better than the more computationally demanding complete active space second-order perturbation theory (CASPT2) with large basis sets and performs even better than CASPT2 with smaller basis sets.

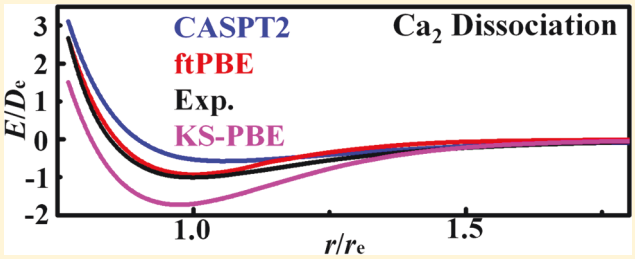

Alkaline earth atoms and their dimers are widely used as trapped ultracold atoms and molecules in their singlet ground states.[1−3] The binding energy of Be_2 is 2.7 kcal/mol.[4] In comparison, Li, which is its neighbor in the periodic table, has a dimer binding energy of 20.4 kcal/mol,[5] which is 8 times larger, and Ne_2 (selected for comparison because Ne is the noble gas in the same row of the periodic table) has a binding energy of 0.08 kcal/mol (32 times smaller).[6] We see that the alkaline earth dimers occupy a middle ground between noble gas dimers and typical covalent bonds. The binding in alkaline earth dimers and clusters has been widely studied and is especially fascinating because of their closed-subshell electronic structure.[7−15]

An especially interesting property of Be_2 is the 2s−2p hybridization.[16] Many studies of alkaline earth dimers have been carried out, especially for Be_2, which in the earliest experimental[17,18] and theoretical[19] investigations was believed to be unstable. Even when later theoretical calculations showed a weak bond for Be_2, controversy remained about whether the equilibrium distance was about 2.5[20−24] or 4.5 Å.[25,26] Experiments have now shown that the equilibrium distance is 2.44−2.45 Å, with a well depth of about 2.66 kcal/mol[4,27,28] Theoretical studies with various wave function methods showed that very high levels such as full configuration interaction (FCI) calculations with large basis sets are required to calculate the binding energy correctly.[29−32]

Of the many studies carried out for heavier alkaline earth dimers,[33−45] we emphasize the calculations done by coupled-cluster theory with single and double excitations and quasiperturbative connected triple excitations, [CCSD(T)],[46] with a perturbative treatment of relativistic effects[47−49] and the basis set extrapolated to the complete basis set (CBS) limit.[50] Reference 50 agrees with experimental values very well for Ca_2 and Sr_2, differing in experiments by no more than 0.06 kcal/mol, and therefore, these results are used as reference values for Ca_2, Sr_2, and Ba_2 in the present work. Radium is the heaviest alkaline earth metal, but there is a lack of experimental data, and we found only two theoretical papers that provide estimated thermodynamic data for Ra_2.[51,52]

In the earliest work, Kohn−Sham density functional theory[53] (KS-DFT) with local exchange−correlation functionals was hard pressed to accurately describe these systems, in part because many local functionals (for example, generalized gradient approximations (GGAs)) do not usually describe van der Waals (vdW) interactions accurately.[54−56] Progress in obtaining better energies for weak interactions by KS-DFT has mainly involved four kinds of strategies: combining KS-DFT with damped dispersion by molecular mechanics,[57,58] introducing nonlocal correlation into the exchange−correlation density functional,[59−64] using parametrized functionals containing kinetic energy density,[65] and using range separation to combine KS-DFT for short interelectronic separations with wave function theory for long interelectronic separations.[66]

Multiconfiguration pair-density functional theory[67] (MC-PDFT) uses on-top density functionals; in current practice these are translated from existing GGA exchange−correlation

Received: December 24, 2018
Accepted: February 4, 2019
Published: February 4, 2019

DOI: 10.1021/acs.jpclett.8b03846
J. Phys. Chem. Lett. 2019, 10, 799−805

Table 1. *M* Diagnostics and Dominant Configurations at the Equilibrium Geometry As Calculated by FV-CASSCF Calculations[a]

		squared coefficient			
	M	$\sigma_{ns}^2\sigma_{ns}^{*2}$	$\sigma_{ns}^2\sigma_{npz}^2$	$\sigma_{ns}^1\sigma_{ns}^{*1}\pi_{npx}^1\pi_{npy}^{*1}$	$\sigma_{ns}^1\sigma_{ns}^{*1}\pi_{npy}^1\pi_{npx}^{*1}$
Be_2	0.27	0.80	0.069	0.024	0.024
Mg_2	0.12	0.86	0.007	0.023	0.023
Ca_2	0.13	0.83	0.022	0.026	0.026
Sr_2	0.12	0.84	0.018	0.025	0.025
Ba_2	0.14	0.83	0.019	0.020	0.020
Ra_2	0.10	0.87	0.010	0.021	0.021

[a]Geometries for Be_2 to Ba_2 are experimental geometries. For Ra_2, the CPO-tPBE, FV-ftPBE, and CPO-ftPBE calculations all give 5.28 Å, and therefore, that distance was used for Ra_2 in this table.

functionals, e.g., tPBE is a translation of the PBE[68] exchange−correlation functional, and ftPBE,[69] which is a full translation of the PBE functional. MC-PDFT calculations have usually been performed using the kinetic energy, density, and on-top density from complete active space self-consistent field[70] (CASSCF) calculations, in which case they may be called CAS-PDFT; reviews are available.[71,72] Here we study whether CASSCF with translated GGAs can describe weak bonding well, even though the untranslated functional does not perform very well in KS-DFT and even though the density functional we use does not involve any of the four strategies mentioned in the previous paragraph.

Computational Methodology. Dissociation energies (D_e) and ground-state equilibrium bond distances (r_e) of Be_2, Mg_2, Ca_2, Sr_2, Ba_2, and Ra_2 were calculated by the two multireference (MR) methods: (i) CAS-PDFT with either the tPBE or the ftPBE on-top functional and (ii) complete active space second-order perturbation theory[73−75] (CASPT2).

We used three basis sets that are designed for calculations that include scalar relativistic effects, ANO-RCC, ANO-RCC-VQZP, and ANO-RCC-VTZP,[76] where ANO-RCC is a very large contracted basis to be denoted AR, ANO-RCC-VQZP is contracted down to valence quadruple-ζ plus polarization and will be denoted ARQ, and ANO-RCC-VTZP is contracted down to valence triple-ζ plus polarization and will be denoted ART. The actual number of primitive and contracted basis functions in each of these basis sets for each of the dimers is given in the SI in Tables S20−S23. The SI also considers nonrelativistic calculations with nonrelativistic basis sets.

The CAS-PDFT and CASPT2 calculations are based on the same CASSCF wave functions. We examined the use of two popular choices for the active space. The first is the widely used full valence (FV) active space, in which the active electrons are all of the valence electrons and the active orbitals are those formed from the valence orbitals of all of the atoms; for alkaline earth dimers, this yields four active electrons in eight active orbitals (σ_{ns}, σ_{ns}^*, σ_{pz}, σ_{pz}^*, π_{px}, π_{px}^*, π_{py}, and π_{py}^* formed primarily by the valence s and p orbitals of the two centers). The second active space, which was tested for only the largest AR basis set, is based on the correlated participating orbitals (CPO) scheme,[77−79] which for alkaline earth dimers involves all occupied bonding and antibonding orbitals plus a correlating orbital for each, and therefore, there are four active electrons in four active orbitals, which are the bonding and antibonding orbitals and a correlating orbital for each, namely, σ_{ns}, σ_{ns}^*, σ_{pz}, and σ_{pz}^* (in previous work, we distinguished three levels of the CPO scheme, but for alkaline earth dimers, they are all the same because there are no occupied nonbonding valence orbitals).

The CASPT2 calculations use a default ionization energy−electron affinity (IPEA) shift of 0.25 au[80] and an imaginary shift of 0.2 au.[81]

We also performed unrestricted KS-DFT with the PBE functional, which is the Kohn−Sham exchange−correlation functional corresponding to the tPBE and ftPBE on-top functionals of MC-PDFT.

A second-order Douglas−Kroll−Hess[82,83] (DKH) relativistic Hamiltonian is used for all of the calculations to account for scalar relativistic effects. All of the calculations were done in Molcas 8.1.[84]

In some of the following discussion, we use a simplified notation: MC-PDFT with the ftPBE and tPBE on-top functionals are simply called ftPBE and tPBE, respectively. Additionally, we use a prefix to indicate an active space, for example, CPO-tPBE and FV-CASPT2. The KS-DFT calculations with the PBE exchange−correlation functional are called KS-PBE.

Multiconfigurational Character. One of the challenges in these alkaline earth dimers is that the multiconfigurational nature of the system is important for describing the character of the bonding. The *M* diagnostic[85] indicates how strongly multiconfigurational a system is. Details of how to calculate *M* diagnostics can be found in ref 85, but a simplified description is that *M* measures the deviations of frontier natural orbital occupation numbers from integers. The *M* diagnostics for the alkaline earth metal dimers at their experimental equilibrium distances can be found in Table 1, and the results show that they are all strongly multiconfigurational systems ($M \geq 0.10$). Although all six dimers are strongly correlated, Be_2 is the most strongly correlated, and Mg_2 and Ra_2 are least strongly correlated.

In order to show which configurations dominate the deviation from a single-configuration wave function, Table 1 shows the dominant configurations in the FV-CASSCF wave function at the equilibrium geometry. The same four configurations have the largest squared coefficients for all six dimers. We observe that a determinant with configuration $\sigma_{ns}^2\sigma_{npz}^2$ plays a much more important role in the wave function for Be_2 than it does for the rest of the dimers, which is consistent with the important role of s−p hybridization in Be_2 that has previously been pointed out by Schmidt et al.[16]

In the CPO-CASSCF calculations, only the first two configurations shown in Table 1 have significant weights; the configuration coefficients are in the SI.

Binding Energies (D_e) for Dimers from Be_2 to Ba_2. The reference values of the bond energies and equilibrium distances are given in Table 2. The MC-PDFT and CASPT2 results calculated with the largest basis set (the AR basis set) using the

DOI: 10.1021/acs.jpclett.8b03846
J. Phys. Chem. Lett. 2019, 10, 799−805

Table 2. Reference Values for Dissociation Energies (D_e, in kcal/mol) and Equilibrium Distances (r_e, in Å)

	D_e	r_e
Be_2	2.66[a]	2.454[a]
Mg_2	1.24[b]	3.890[b]
Ca_2	3.13[c]	4.287[c]
Sr_2	3.02[c]	4.663[c]
Ba_2	3.87[c]	4.972[c]

[a]These results are from the most recent experimental value (2.658 ± 0.006 kcal/mol) in ref 4. [b]These results are from experimental values in ref 33. [c]The results are from high-level theoretical calculations in ref 50.

two active spaces are given in Table 3. We consider four mean unsigned errors (MUEs) for MC-PDFT; these MUEs correspond to the four possible combinations of two active spaces and two on-top density functionals. We also give two MUEs for CASPT2; they correspond to the two active spaces. For the bond energy, three of the four MUEs for MC-PDFT are smaller than the better of the two CASPT2 MUEs, and the fourth is the same. This is a key finding of the present study. Table 3 also shows mean signed errors (MSEs) and standard deviations.

Note that the ftPBE calculations overestimate the bond energy for Be_2 and Ba_2, underestimate it for Mg_2, and either overestimate it or underestimate it, depending on the active space, for Ca_2 and Sr_2. The smallest errors of the ftPBE calculations are achieved for Mg_2 and Ba_2, and the largest error is for Be_2.

Equilibrium Internuclear Distances (r_e) for Dimers from Be_2 to Ba_2. Table 2 also shows the accuracy that can be achieved for the bond distances. Again we consider four MUEs for MC-PDFT; these MUEs correspond to the four possible combinations of two active spaces and two on-top density functionals. We also give two MUEs for CASPT2; they correspond to the two active spaces. For the equilibrium distance, all four MUEs for MC-PDFT are smaller than either of the CASPT2 MUEs. This is another important finding of the present study.

Larger Active Spaces. We also explored bigger active spaces for MC-PDFT calculations on Be_2, and the results are in Table S2 in the SI. The performance is somewhat worse with the larger active spaces. This result is consistent with a previous detailed study on H_2 where we found that very large active spaces can degrade the result.[86] In general, we recommend that the active space should be large enough to include the dominant static correlation but not significantly larger. Therefore, it is encouraging that we get generally good results with the two standard active space choices in Table 3.

Basis Set Dependence. The MC-PDFT and CASPT2 results calculated with the contracted basis sets using the FV active space are given in Table 4. With smaller valence basis sets, namely, ARQ and ART, a general trend is found that the results of CASPT2 change more (as compared to the larger AR basis set) than do the ftPBE calculations. Comparison of Tables 4 and 3 shows that the accuracy of CASPT2 degrades significantly with smaller basis sets, which is not surprising because of the slow convergence of perturbation theory with basis set size. For ftPBE, we see a smaller degradation in bond energies and no degradation in bond distances. Thus, MC-PDFT retains its accuracy comparatively better with basis sets that would be more practical for larger systems.

Comparison to KS-DFT. The KS-PBE results are given in Table 5. The KS-DFT bond energies with the parent GGA are, on average, much less accurate than MC-PDFT or CASPT2. We see that MC-PDFT with either active space gives the most accurate bond distances, followed by CPO-CASPT2, then KS-PBE, and at last FV-CASPT2.

Table 3. Dissociation Energy, Equilibrium Distance, Mean Signed Error (MSE), Mean Unsigned Error (MUE), and Standard Deviation (StdDev) for Calculations with the Large AR Basis Set[a]

		ftPBE		tPBE		CASPT2	
active space	molecule	D_e	r_e	D_e	r_e	D_e	r_e
FV	Be_2	3.58	2.404	1.42	2.436	0.00[b]	2.554
	Mg_2	0.49	3.800	−0.10[b]	4.242	0.60	4.313
	Ca_2	2.64	4.284	1.56	4.376	1.81	4.536
	Sr_2	2.76	4.657	1.77	4.752	1.94	4.855
	Ba_2	3.89	4.960	2.80	5.038	2.88	5.102
	Ra_2	2.34	5.275	1.48	5.379	1.82	5.521
	MSE	−0.11	−0.032	−1.3	0.12	−1.3	0.22
	MUE	0.49	0.032	1.3	0.12	1.3	0.22
	StdDev[c]	0.64	0.037	0.18	0.14	0.78	0.13
CPO	Be_2	4.09	2.440	4.44	2.375	4.50	2.423
	Mg_2	1.00	3.767	0.96	3.768	2.83	4.068
	Ca_2	3.46	4.304	3.12	4.314	4.39	4.439
	Sr_2	3.58	4.682	3.27	4.682	4.53	4.806
	Ba_2	4.80	4.983	4.52	4.975	5.73	5.056
	Ra_2	3.11	5.276	2.79	5.282	4.24	5.410
	MSE	0.60	−0.018	0.48	−0.030	1.6	0.11
	MUE	0.70	0.037	0.59	0.050	1.6	0.12
	StdDev[c]	0.63	0.060	0.80	0.066	0.25	0.084

[a]All energies in this table are in kcal/mol, and all distances are in Å. Error statistics are based on Be_2−Ba_2 because accurate results are not available for Ra_2. [b]These nonbonding results correspond to local minima on potential energy curves. See Figure 2b as an example where CASPT2 fails. See also refs 25 and 26 for similar results, consistent with the difficulty in studying Be_2. [c]The standard deviation in the tables is the standard deviation of the unsigned errors from their mean.

DOI: 10.1021/acs.jpclett.8b03846
J. Phys. Chem. Lett. 2019, 10, 799−805

Table 4. Dissociation Energy, Equilibrium Distance, Mean Signed Error (MSE), Mean Unsigned Error (MUE), and Standard Deviation (StdDev) for Calculations with the Smaller Basis Sets[a]

		ART		ARQ	
method	molecule	D_e	r_e	D_e	r_e
ftPBE	Be_2	3.30	2.435	3.56	2.412
	Mg_2	0.40	3.855	0.47	3.812
	Ca_2	2.44	4.303	2.55	4.296
	Sr_2	2.53	4.676	2.70	4.669
	Ba_2	3.68	5.000	3.86	4.970
	MSE	−0.31	0.001	−0.16	−0.021
	MUE	0.57	0.022	0.52	0.027
	StdDev[b]	0.59	0.026	0.66	0.038
CASPT2	Be_2	−0.56	2.513	−0.24	2.630
	Mg_2	0.56	4.690	0.64	4.397
	Ca_2	1.13	4.790	1.41	4.653
	Sr_2	1.17	5.199	1.69	4.972
	Ba_2	3.07	5.154	3.88	5.016
	MSE	−1.71	0.42	−1.31	0.28
	MUE	1.71	0.42	1.31	0.28
	StdDev[b]	1.03	0.30	1.11	0.18

[a]All energies in this table are in kcal/mol, and all distances are in Å. [b]The standard deviation in the tables is the standard deviation of the unsigned errors from their mean.

Table 5. Dissociation Energy, Equilibrium Distance, Mean Signed Error (MSE), Mean Unsigned Error (MUE), and Standard Deviation (StdDev) for Calculations with KS-DFT Using the PBE Exchange−Correlation Functional[a]

	ART		ARQ		AR	
	D_e	r_e	D_e	r_e	D_e	r_e
Be_2	9.7	2.458	9.8	2.438	9.8	2.431
Mg_2	3.2	3.518	3.2	3.512	3.2	3.510
Ca_2	5.2	4.197	5.3	4.188	5.4	4.171
Sr_2	4.7	4.556	4.8	4.555	4.9	4.544
Ba_2	6.4	4.863	6.6	4.845	6.6	4.845
Ra_2	3.6	5.197	3.5	5.205	3.8	5.172
MSE	3.1	−0.14	3.2	−0.15	3.2	−0.15
MUE	3.1	0.14	3.2	0.15	3.2	0.15
StdDev[b]	2.3	0.14	2.3	0.14	2.2	0.13

[a]All energies in this table are in kcal/mol, and all distances are in Å. Error statistics are based on Be_2−Ba_2 because accurate results are not available for Ra_2. [b]The standard deviation in the tables is the standard deviation of the unsigned errors from their mean.

Potential Energy Curves. Figure 1 shows dissociation curves of Mg_2 and Ca_2 by FV-ftPBE, FV-CASPT2, and KS-PBE as compared to the experimental curve from refs 87 and 88, respectively. (The potential energy curve for Be_2 is shown in Figure 2, discussed below, and the potential energy curves for all six dimers are given in tabular form in Tables S18−S23 in the SI. We did not find experimental potential energy curves for Sr_2, Ba_2, or Ra_2.) Figure 1 shows that the FV-ftPBE curve agrees with the experiment very well for both equilibrium distances and dissociation energies, but it is underestimated for the long-range tail of the potential, which may be attributed to underestimation of dispersion energy contributions.

The potential energy curves for Be_2 are shown in Figure 2 near the equilibrium internuclear distance; this figure shows that the ftPBE results are well converged at ARQ, but for this

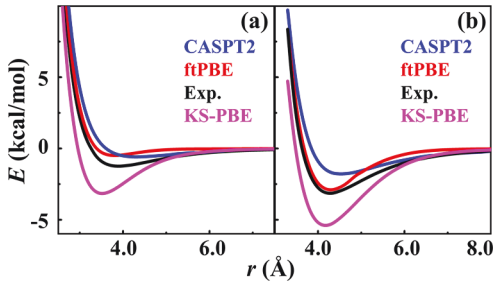

Figure 1. Dissociation curves for (a) Mg_2 and (b) Ca_2 by FV-CASPT2, FV-ftPBE, and KS-PBE using the AR basis set. Also shown is the experimental curve (labeled "Exp.").

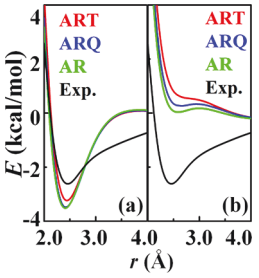

Figure 2. Potential energy curve (zero at 20 Å) of Be_2 near equilibrium by (a) FV-ftPBE and (b) FV-CASPT2, using the ART, ARQ, and AR basis sets. Also shown is the experimental curve (abbreviated Exp.).[4]

basis set, the CASPT2 calculations still have a significant difference from the AR curves.

Performance of Other On-Top Functionals. In Tables S4−S6, we present results for other on-top translated and fully translated functionals[89] compared with each other and compared with their untranslated KS analogues, namely, KS-revPBE[90] and KS-OPBE[68,91] together with their translated or fully translated versions. We found that fully translated functionals are usually more accurate than their corresponding translated ones, and the fully translated functionals have better performance than their corresponding KS parent functionals. One possible reason for the improved performance of the ft functionals is that they include the gradient of the on-top density.

MP2 vs CASPT2. One may ask whether the improved performance of ftPBE or tPBE over KS-PBE originates from MC-PDFT being able to handle multiconfigurational systems better. The *M* diagnostics presented above show that these systems are inherently multiconfigurational (i.e., strongly correlated), but it is also useful to consider another aspect of MR character, namely, the deviation of CASPT2 based on CASSCF from single-configuration Møller−Plesset perturbation theory[92,93] (MP2) based on a restricted Hartree−Fock calculation. The MP2 results are given in Table S8 in the SI. When using the AR basis set, we find, unexpectedly, that MP2 performs better than CASPT2. This demonstrates how difficult it is to identify sources of errors in approximate calculations. There is a subtle interplay between all of the approximations, and there is some cancellation of errors, and for weak interactions, this can subvert any simple attempt to divide the errors into categories.

Core Correlation. All of the CASPT2 calculations reported here and in the SI make the frozen-core approximation. The SI contains a comparison of full MP2, denoted as MP2(Full),

DOI: 10.1021/acs.jpclett.8b03846
J. Phys. Chem. Lett. 2019, 10, 799−805

which includes excitation of all core orbitals, and frozen-core MP2, denoted FC-MP2, which does not allow excitations of core orbitals. The latter is important because all of the CASPT2 calculations reported here and in the SI make the frozen-core approximation. The comparison is in Tables S7 and S8, and it shows that sometimes core correlation improves the results and sometimes it makes them worse. This is perhaps not surprising because it is known that core polarization is particularly important in group 2 of the periodic table.[94−96] One advantage of density functional methods over wave function methods is that density functional methods always include core correlation, at least to the extent allowed by the basis set.

Diffuse Basis Functions and Core Polarization Basis Functions. Tables S9−S12 present additional tests for Be_2 and Mg_2, showing that the results are not sensitive to diffuse functions or to the core polarization functions in the basis sets.

D_e and r_e for Ra_2. Because there is no accurate experiment available for Ra_2, we also made ftPBE calculations for Ra_2. The results given by FV-ftPBE and CPO-tPBE are in quite good agreement with some previous calculations. A CCSD(T) calculation using exact two-component[97,98] (X2C) theory for the relativistic effect gave 2.6 kcal/mol for D_e and 5.324 Å for r_e.[52] A CASPT2 calculation using an active space with 4 electrons in 16 orbitals and the AR basis set gave 1.82 kcal/mol for D_e and 5.478 Å for r_e.[51] The data are in a good agreement with our FV-CASPT2 calculation. The ftPBE results are close to the CCSD(T) result for both dissociation energy and bond distance.

Concluding Remarks. Alkaline earth dimers embody two of the most challenging problems in quantum chemistry—weak interactions and strongly correlated systems. The present study shows that MC-PDFT provides improved accuracy as compared to KS-DFT and CASPT2 for weak bonds in metal dimers. Furthermore, MC-PDFT has the advantage of having less dependence on basis sets than one finds for wave function methods like MP2 or CASPT2. This reduced basis set dependence is usually an advantage of density functional methods over methods that must explicitly build the electron−electron cusp into the wave function in order to accurately approximate the dynamic correlation energy, and MC-PDFT provides a way to take advantage of this in a setting that includes multiconfigurational effects in the representation of the electron density.

■ ASSOCIATED CONTENT

Supporting Information

The Supporting Information is available free of charge on the ACS Publications website at DOI: 10.1021/acs.jpclett.8b03846.

Performance of MC-PDFT on Be_2 with larger active spaces, dissociation energies calculated by MP2 with and without core correlation and by KS-revPBE, trevPBE, ftrevPBE, KS-OPBE, tOPBE, and ftOPBE, dissociation energies of Be_2 and Mg_2 using correlation-consistent basis sets, most diffuse s functions in correlation-consistent basis sets with and without augmentation and in ANO basis sets, absolute energies of ftPBE and CASPT2 calculations for all of the alkaline earth metal dimers with the AR basis set, and numbers of primitive and contracted basis functions in AR, ARQ, and ART basis sets (PDF)

■ AUTHOR INFORMATION

Corresponding Authors

*E-mail: gagliard@umn.edu.
*E-mail: truhlar@umn.edu.

ORCID

Jie J. Bao: 0000-0003-0197-3405
Laura Gagliardi: 0000-0001-5227-1396
Donald G. Truhlar: 0000-0002-7742-7294

Notes

The authors declare no competing financial interest.

■ ACKNOWLEDGMENTS

This work is supported in part by the National Science Foundation under Grant No. CHE−1464536.

■ REFERENCES

(1) Kotochigova, S.; Zelevinsky, T.; Ye, J. Prospects for application of ultracold Sr_2 molecules in precision measurements. *Phys. Rev. A: At., Mol., Opt. Phys.* **2009**, *79*, 012504.
(2) De, S.; Dammalapati, U.; Jungmann, K.; Willmann, L. Magneto-optical trapping of barium. *Phys. Rev. A: At., Mol., Opt. Phys.* **2009**, *79*, 041402.
(3) Dammalapati, U.; Norris, I.; Burrows, C.; Arnold, A. S.; Riis, E. Spectroscopy and isotope shifts of the 4s3d $^1D_2$−4s5p $^1P_1$ repumping transition in magneto-optically trapped calcium atoms. *Phys. Rev. A: At., Mol., Opt. Phys.* **2010**, *81*, 023424.
(4) Merritt, J. M.; Bondybey, V. E.; Heaven, M. C. Beryllium dimer−caught in the act of bonding. *Science* **2009**, *324*, 1548−1551.
(5) Maniero, A. M.; Acioli, P. H. Full configuration interaction pseudopotential determination of the ground-state potential energy curves of Li_2 and LiH. *Int. J. Quantum Chem.* **2005**, *103*, 711−717.
(6) Aziz, R. A.; Slaman, M. J. The Ne-Ne interatomic potential revisited. *Chem. Phys.* **1989**, *130*, 187−194.
(7) Khanna, S. N.; Reuse, F.; Buttet, J. Stability and observability of charged beryllium clusters. *Phys. Rev. Lett.* **1988**, *61*, 535−538.
(8) Kumar, V.; Car, R. Structure, growth, and bonding nature of Mg clusters. *Phys. Rev. B: Condens. Matter Mater. Phys.* **1991**, *44*, 8243−8255.
(9) Duanmu, K.; Roberto-Neto, O.; Machado, F. B. C.; Hansen, J. A.; Shen, J.; Piecuch, P.; Truhlar, D. G. Geometries, Binding Energies, Ionization Potentials, and Electron Affinities of Metal Clusters: Mg_nO, ± 1, $_n$ = 1−7. *J. Phys. Chem. C* **2016**, *120*, 13275−13286.
(10) Mirick, J. W.; Chien, C.-H.; Blaisten-Barojas, E. Electronic structure of calcium clusters. *Phys. Rev. A: At., Mol., Opt. Phys.* **2001**, *63*, 023202.
(11) Wang, G. M.; Blaisten-Barojas, E.; Roitberg, A. E.; Martin, T. P. Strontium clusters: Many-body potential, energetics, and structural transitions. *J. Chem. Phys.* **2001**, *115*, 3640−3646.
(12) Wang, Y.; Flad, H.-J.; Dolg, M. Ab initio study of structure and bonding of strontium clusters. *J. Phys. Chem. A* **2000**, *104*, 5558−5567.
(13) Boutou, V.; Allouche, A. R.; Spiegelmann, F.; Chevaleyre, J.; Frécon, M. A. Predictions of geometrical structures and ionization potentials for small barium clusters Ba. *Eur. Phys. J. D* **1998**, *2*, 63−73.
(14) Ruzsinszky, A.; Perdew, J. P.; Csonka, G. I. Binding energy curves from nonempirical density functionals II. van der Waals bonds in rare-gas and alkaline-earth diatomics. *J. Phys. Chem. A* **2005**, *109* (48), 11015−11021.
(15) Zhao, Y.; Truhlar, D. G. Comparative DFT study of van der Waals complexes: Rare-gas dimers, alkaline-earth dimers, zinc dimer, and zinc-rare-gas dimers. *J. Phys. Chem. A* **2006**, *110*, 5121−5129.
(16) Schmidt, M. W.; Ivanic, J.; Ruedenberg, K. Electronic structure analysis of the ground-state potential energy curve of Be_2. *J. Phys. Chem. A* **2010**, *114*, 8687−8696.
(17) Herzberg, G. Zum Aufbau der zweiatomigen Moleküle. *Eur. Phys. J. A* **1929**, *57*, 601−630.

DOI: 10.1021/acs.jpclett.8b03846
J. Phys. Chem. Lett. 2019, 10, 799−805

(18) Herzberg, L. Über ein neues Bandensystem des Berylliumoxyds und die Struktur des Be O-Moleküls. *Eur. Phys. J. A* **1933**, *84*, 571−592.
(19) Bender, C. F.; Davidson, E. R. Theoretical calculation of the potential curves of the Be_2 Molecule. *J. Chem. Phys.* **1967**, *47*, 4972−4978.
(20) Liu, B.; McLean, A. D. Ab initio potential curve for Be_2 ($^1\Sigma_g^+$) from the interacting correlated fragments method. *J. Chem. Phys.* **1980**, *72*, 3418−3419.
(21) Lengsfield, B. H.; McLean, A. D.; Yoshimine, M.; Liu, B. The binding energy of the ground state of Be_2. *J. Chem. Phys.* **1983**, *79*, 1891−1895.
(22) Stärck, J.; Meyer, W. The ground state potential of the beryllium dimer. *Chem. Phys. Lett.* **1996**, *258*, 421−426.
(23) Schautz, F.; Flad, H. J.; Dolg, M. Quantum Monte Carlo study of Be_2 and group 12 dimers M_2 (M = Zn, Cd, Hg). *Theor. Chem. Acc.* **1998**, *99*, 231−240.
(24) Jordan, K. D. Electronic structure of small metal clusters. I. Anions of Be_2, Be_3, and Be_4. *J. Chem. Phys.* **1999**, *67*, 4027.
(25) Chiles, R. A.; Dykstra, C. E. An electron pair operator approach to coupled cluster wave functions. Application to He_2, Be_2, and Mg_2 and comparison with CEPA methods. *J. Chem. Phys.* **1981**, *74*, 4544−4556.
(26) Lee, Y. S.; Bartlett, R. J. A study of Be_2 with many-body perturbation theory and a coupled-cluster method including triple excitations. *J. Chem. Phys.* **1984**, *80*, 4371−4377.
(27) Brom, J. M., Jr; Hewett, W. D., Jr; Weltner, W., Jr Optical spectra of Be atoms and Be_2 molecules in rare gas matrices. *J. Chem. Phys.* **1975**, *62*, 3122−3130.
(28) Patkowski, K.; Spirko, V.; Szalewicz, K. On the elusive twelfth vibrational state of beryllium dimer. *Science* **2009**, *326*, 1382−1384.
(29) Blomberg, M. R. A.; Siegbahn, P. E. M. Beryllium dimer, a critical test case of MBPT and CI methods. *Int. J. Quantum Chem.* **1978**, *14*, 583−592.
(30) Schmidt, M. W.; Ivanic, J.; Ruedenberg, K. Electronic structure analysis of the ground-state potential energy curve of Be_2. *J. Phys. Chem. A* **2010**, *114*, 8687−8696.
(31) Evangelisti, S.; Bendazzoli, G. L.; Gagliardi, L. Full configuration interaction calculations on Be_2. *Chem. Phys.* **1994**, *185*, 47−56.
(32) Magoulas, I.; Bauman, N. P.; Shen, J.; Piecuch, P. Application of the CC($P;Q$) hierarchy of coupled-cluster methods to the beryllium dimer. *J. Phys. Chem. A* **2018**, *122*, 1350−1368.
(33) Balfour, W. J.; Douglas, A. E. Absorption spectrum of the Mg_2 molecule. *Can. J. Phys.* **1970**, *48*, 901−914.
(34) Vidal, C. R.; Scheingraber, H. Determination of diatomic molecular constants using an inverted perturbation approach. *J. Mol. Spectrosc.* **1977**, *65*, 46−64.
(35) Purvis, G. D.; Bartlett, R. J. The potential energy curve for the $X\ ^1\Sigma_g^+$ state of Mg_2 calculated with many-body perturbation theory. *J. Chem. Phys.* **1978**, *68*, 2114−2124.
(36) Partridge, H.; Bauschlicher, C. W.; Pettersson, L. G. M.; McLean, A. D.; Liu, B.; Yoshimine, M.; Komornicki, A. On the dissociation energy of Mg_2. *J. Chem. Phys.* **1990**, *92*, 5377−5383.
(37) Li, P.; Xie, W.; Tang, K. T. The van der Waals potential of the magnesium dimer. *J. Chem. Phys.* **2010**, *133*, 084308.
(38) Vidal, C. R. The molecular constants and potential energy curves of the Ca_2 $A\ ^1\Sigma_u^+ - X\ ^1\Sigma_g^+$ system from laser induced fluorescence. *J. Chem. Phys.* **1980**, *72*, 1864−1874.
(39) Allard, O.; Samuelis, C.; Pashov, A.; Knöckel, H.; Tiemann, E. Experimental study of the Ca_2 $^1S + {}^1S$ asymptote. *Eur. Phys. J. B* **2003**, *26*, 155−164.
(40) Yang, D. D.; Li, P.; Tang, K. T. The ground state van der Waals potentials of the calcium dimer and calcium rare-gas complexes. *J. Chem. Phys.* **2009**, *131*, 154301.
(41) Bergeman, T.; Liao, P. F. Photoassociation, photoluminescence, and collisional dissociation of the Sr_2 dimer. *J. Chem. Phys.* **1980**, *72*, 886−898.
(42) Stein, A.; Knöckel, H.; Tiemann, E. Fourier-transform spectroscopy of Sr_2 and revised ground-state potential. *Phys. Rev. A: At., Mol., Opt. Phys.* **2008**, *78*, 042508.
(43) Yin, G. P.; Li, P.; Tang, K. T. The ground state van der Waals potentials of the strontium dimer and strontium rare-gas complexes. *J. Chem. Phys.* **2010**, *132*, 074303.
(44) Allouche, A. R.; Aubert-Frécon, M.; Nicolas, G.; Spiegelmann, F. Theoretical study of the electronic structure of the Ba_2 molecule. *Chem. Phys.* **1995**, *200*, 63−77.
(45) Schäfer, S.; Mehring, M.; Schäfer, R.; Schwerdtfeger, P. Polarizabilities of Ba and Ba_2: Comparison of molecular beam experiments with relativistic quantum chemistry. *Phys. Rev. A: At., Mol., Opt. Phys.* **2007**, *76*, 052515.
(46) Raghavachari, K.; Trucks, G. W.; Pople, J. A.; Head-Gordon, M. A fifth-order perturbation comparison of electron correlation theories. *Chem. Phys. Lett.* **1989**, *157*, 479−483.
(47) Kutzelnigg, W. Perturbation theory of relativistic corrections. *Z. Phys. D: At., Mol. Clusters* **1989**, *11*, 15−28.
(48) Kutzelnigg, W. Perturbation theory of relativistic corrections. *Z. Phys. D: At., Mol. Clusters* **1990**, *15*, 27−50.
(49) Stopkowicz, S.; Gauss, J. Relativistic corrections to electrical first-order properties using direct perturbation theory. *J. Chem. Phys.* **2008**, *129*, 164119.
(50) Yang, D.-D.; Wang, F. Theoretical investigation for spectroscopic constants of ground-state alkaline-earth dimers with high accuracy. *Theor. Chem. Acc.* **2012**, *131*, 1117.
(51) Veryazov, V.; Widmark, P.-O.; Roos, B. O. Relativistic atomic natural orbital type basis sets for the alkaline and alkaline-earth atoms applied to the ground-state potentials for the corresponding dimers. *Theor. Chem. Acc.* **2004**, *111*, 345−351.
(52) Teodoro, T. Q.; Haiduke, R. L.; Dammalapati, U.; Knoop, S.; Visscher, L. The ground-state potential energy curve of the radium dimer from relativistic coupled cluster calculations. *J. Chem. Phys.* **2015**, *143*, 084307.
(53) Kohn, W.; Sham, L. J. Self-consistent equations including exchange and correlation effects. *Phys. Rev.* **1965**, *140*, A1133−A1138.
(54) Kristyán, S.; Pulay, P. Can (semi)local density functional theory account for the London dispersion forces? *Chem. Phys. Lett.* **1994**, *229*, 175−180.
(55) Pérez-Jordá, J.; Becke, A. D. A density-functional study of van der Waals forces: rare gas diatomics. *Chem. Phys. Lett.* **1995**, *233*, 134−137.
(56) Kohn, W.; Meir, Y.; Makarov, D. E. van der Waals energies in density functional theory. *Phys. Rev. Lett.* **1998**, *80*, 4153−4156.
(57) Wu, Q.; Yang, W. Empirical correction to density functional theory for van der Waals interactions. *J. Chem. Phys.* **2002**, *116*, 515−524.
(58) Grimme, S.; Antony, J.; Ehrlich, S.; Krieg, H. A consistent and accurate ab initio parametrization of density functional dispersion correction (DFT-D) for the 94 elements H-Pu. *J. Chem. Phys.* **2010**, *132*, 154104.
(59) Zhao, Y.; Lynch, B. J.; Truhlar, D. G. Doubly hybrid meta DFT: New multi-coefficient correlation and density functional methods for thermochemistry and thermochemical kinetics. *J. Phys. Chem. A* **2004**, *108*, 4786−4791.
(60) Cooper, V. R.; Thonhauser, T.; Langreth, D. C. An application of the van der Waals density functional: Hydrogen bonding and stacking interactions between nucleobases. *J. Chem. Phys.* **2008**, *128*, 204102.
(61) Tarnopolsky, A.; Karton, A.; Sertchook, R.; Vuzman, D.; Martin, J. M. L. Double-Hybrid Functionals for Thermochemical Kinetics. *J. Phys. Chem. A* **2008**, *112*, 3−8.
(62) Zhang, Y.; Xu, X.; Goddard, W. A., 3rd. Doubly hybrid density functional for accurate descriptions of nonbond interactions, thermochemistry, and thermochemical kinetics. *Proc. Natl. Acad. Sci. U. S. A.* **2009**, *106*, 4963−4968.
(63) Vydrov, O. A.; Van Voorhis, T. Benchmark assessment of the accuracy of several van der Waals density functionals. *J. Chem. Theory Comput.* **2012**, *8*, 1929−1934.

DOI: 10.1021/acs.jpclett.8b03846
J. Phys. Chem. Lett. 2019, 10, 799−805

(64) Klimes, J.; Michaelides, A. Perspective: Advances and challenges in treating van der Waals dispersion forces in density functional theory. *J. Chem. Phys.* **2012**, *137*, 120901.
(65) Zhao, Y.; Truhlar, D. G. Applications and validations of the Minnesota density functionals. *Chem. Phys. Lett.* **2011**, *502*, 1−13.
(66) Goll, E.; Werner, H.-J.; Stoll, H.; Leininger, T.; Gori-Giorgi, P.; Savin, A. A short-range gradient-corrected spin density functional in combination with long-range coupled-cluster methods: Application to alkali-metal rare-gas dimers. *Chem. Phys.* **2006**, *329*, 276−282.
(67) Li Manni, G.; Carlson, R. K.; Luo, S.; Ma, D.; Olsen, J.; Truhlar, D. G.; Gagliardi, L. Multiconfiguration pair-density functional theory. *J. Chem. Theory Comput.* **2014**, *10*, 3669−3680.
(68) Perdew, J. P.; Burke, K.; Ernzerhof, M. Generalized gradient approximation made simple. *Phys. Rev. Lett.* **1996**, *77*, 3865−3868.
(69) Carlson, R. K.; Truhlar, D. G.; Gagliardi, L. Multiconfiguration pair-density functional theory: a fully translated gradient approximation and its performance for transition metal dimers and the spectroscopy of $Re_2Cl_8^{2-}$. *J. Chem. Theory Comput.* **2015**, *11*, 4077−4085.
(70) Roos, B. O.; Taylor, P. R.; Siegbahn, P. E. M. A complete active space SCF method (CASSCF) using a density matrix formulated super-CI approach. *Chem. Phys.* **1980**, *48*, 157−173.
(71) Gagliardi, L.; Truhlar, D. G.; Li Manni, G.; Carlson, R. K.; Hoyer, C. E.; Bao, J. L. Multiconfiguration pair-density functional theory: A New way to treat strongly correlated systems. *Acc. Chem. Res.* **2017**, *50*, 66−73.
(72) Ghosh, S.; Verma, P.; Cramer, C. J.; Gagliardi, L.; Truhlar, D. G. Combining wave function methods with density functional theory for excited states. *Chem. Rev.* **2018**, *118*, 7249−7292.
(73) Roos, B. O.; Linse, P.; Siegbahn, P. E. M.; Blomberg, M. R. A. A simple method for the evaluation of the second-order-perturbation energy from external double-excitations with a CASSCF reference wavefunction. *Chem. Phys.* **1982**, *66*, 197−207.
(74) Andersson, K.; Malmqvist, P. A.; Roos, B. O.; Sadlej, A. J.; Wolinski, K. Second-order perturbation theory with a CASSCF reference function. *J. Phys. Chem.* **1990**, *94*, 5483−5488.
(75) Andersson, K.; Malmqvist, P. Å.; Roos, B. O. Second-order perturbation theory with a complete active space self-consistent field reference function. *J. Chem. Phys.* **1992**, *96*, 1218−1226.
(76) Roos, B. O.; Lindh, R.; Malmqvist, P. A.; Veryazov, V.; Widmark, P. O. Main group atoms and dimers studied with a new relativistic ANO basis set. *J. Phys. Chem. A* **2004**, *108*, 2851−2858.
(77) Tishchenko, O.; Zheng, J.; Truhlar, D. G. Multireference model chemistries for thermochemical kinetics. *J. Chem. Theory Comput.* **2008**, *4*, 1208−1219.
(78) Bao, J. L.; Sand, A.; Gagliardi, L.; Truhlar, D. G. Correlated-participating-orbitals pair-density functional method and application to multiplet energy splittings of main-group divalent radicals. *J. Chem. Theory Comput.* **2016**, *12*, 4274−4283.
(79) Bao, J. L.; Odoh, S. O.; Gagliardi, L.; Truhlar, D. G. Predicting bond dissociation energies of transition-metal compounds by multiconfiguration pair-density functional theory and second-order perturbation theory based on correlated participating orbitals and separated pairs. *J. Chem. Theory Comput.* **2017**, *13*, 616−626.
(80) Ghigo, G.; Roos, B. O.; Malmqvist, P.-Å. A modified definition of the zeroth-order Hamiltonian in multiconfigurational perturbation theory (CASPT2). *Chem. Phys. Lett.* **2004**, *396*, 142−149.
(81) Forsberg, N.; Malmqvist, P. A. Multiconfiguration perturbation theory with imaginary level shift. *Chem. Phys. Lett.* **1997**, *274*, 196−204.
(82) Douglas, M.; Kroll, N. M. Quantum electrodynamical corrections to the fine structure of helium. *Ann. Phys.* **1974**, *82*, 89−155.
(83) Hess, B. A. Relativistic electronic-structure calculations employing a two-component no-pair formalism with external-field projection operators. *Phys. Rev. A: At., Mol., Opt. Phys.* **1986**, *33*, 3742−3748.
(84) Aquilante, F.; Autschbach, J.; Carlson, R. K.; Chibotaru, L. F.; Delcey, M. G.; De Vico, L.; Fdez. Galvan, I.; Ferre, N.; Frutos, L. M.; Gagliardi, L.; Garavelli, M.; Giussani, A.; Hoyer, C. E.; Li Manni, G.; Lischka, H.; Ma, D.; Malmqvist, P. A.; Muller, T.; Nenov, A.; Olivucci, M.; Pedersen, T. B.; Peng, D.; Plasser, F.; Pritchard, B.; Reiher, M.; Rivalta, I.; Schapiro, I.; Segarra-Marti, J.; Stenrup, M.; Truhlar, D. G.; Ungur, L.; Valentini, A.; Vancoillie, S.; Veryazov, V.; Vysotskiy, V. P.; Weingart, O.; Zapata, F.; Lindh, R. Molcas 8: New capabilities for multiconfigurational quantum chemical calculations across the periodic table. *J. Comput. Chem.* **2016**, *37*, 506−541.
(85) Tishchenko, O.; Zheng, J.; Truhlar, D. G. Multireference model chemistries for thermochemical kinetics. *J. Chem. Theory Comput.* **2008**, *4*, 1208.
(86) Sharma, P.; Truhlar, D. G.; Gagliardi, L. Active Space Dependence in Multiconfiguration Pair-Density Functional Theory. *J. Chem. Theory Comput.* **2018**, *14*, 660−669.
(87) Tiesinga, E.; Kotochigova, S.; Julienne, P. S. Scattering length of the ground-state Mg + Mg collision. *Phys. Rev. A: At., Mol., Opt. Phys.* **2002**, *65*, 042722.
(88) Allard, O.; Pashov, A.; Knöckel, H.; Tiemann, E. Ground-state potential of the Ca dimer from Fourier-transform spectroscopy. *Phys. Rev. A: At., Mol., Opt. Phys.* **2002**, *66*, 042503.
(89) Hoyer, C. E.; Ghosh, S.; Truhlar, D. G.; Gagliardi, L. Multiconfiguration pair-density functional theory is as accurate as CASPT2 for electronic excitation. *J. Phys. Chem. Lett.* **2016**, *7*, 586−591.
(90) Zhang, Y.; Yang, W. Comment on "Generalized gradient approximation made simple. *Phys. Rev. Lett.* **1998**, *80*, 890.
(91) Handy, N. C.; Cohen, A. J. Left-right correlation energy. *Mol. Phys.* **2001**, *99*, 403−412.
(92) Møller, C.; Plesset, M. S. Note on an approximation treatment for many-electron systems. *Phys. Rev.* **1934**, *46*, 618−622.
(93) Bartlett, R. J.; Purvis, G. D. Many-body perturbation theory, coupled-pair many-electron theory, and the importance of quadruple excitations for the correlation problem. *Int. J. Quantum Chem.* **1978**, *14*, 561−581.
(94) Martin, J. M. L.; Sundermann, A.; Fast, P. L.; Truhlar, D. G. Thermochemical analysis of core correlation and scalar relativistic effects on molecular atomization energies. *J. Chem. Phys.* **2000**, *113*, 1348−1358.
(95) Sullivan, M. B.; Iron, M. A.; Redfern, P. C.; Martin, J. M. L.; Curtiss, L. A.; Radom, L. Heats of formation of alkali metal and alkaline earth metal oxides and hydroxides: Surprisingly demanding targets for high-level ab initio procedures. *J. Phys. Chem. A* **2003**, *107*, 5617−5630.
(96) Yu, H.; Truhlar, D. G. Components of the bond energy in polar diatomic molecules, radicals, and ions formed by group-1 and group-2 metal atoms. *J. Chem. Theory Comput.* **2015**, *11*, 2968−2983.
(97) Barysz, M.; Sadlej, A. J. Two-component methods of relativistic quantum chemistry: from the Douglas−Kroll approximation to the exact two-component formalism. *J. Mol. Struct.: THEOCHEM* **2001**, *573*, 181−200.
(98) Liu, W.; Peng, D. Exact two-component Hamiltonians revisited. *J. Chem. Phys.* **2009**, *131*, 031104.

DOI: 10.1021/acs.jpclett.8b03846
J. Phys. Chem. Lett. 2019, 10, 799−805